Acta Societatis Botanicorum Poloniae

DOI: 10.5586/asbp.3534

Publication history
Received: 2016-12-26
Accepted: 2016-12-30
Published: 2016-12-31

Handling editors
Beata Zagórska-Marek, Faculty of Biological Sciences, University of Wrocław, Poland
Przemysław Prusinkiewicz, Faculty of Science, University of Calgary, Canada

Authors' contributions
CG performed the analysis of the artichoke and birch catkin, SD the remaining ones; CG performed the numerical simulations; SD and CG wrote the article

Funding
GC was partially supported by an NSF collaborative grants #0540740 for this work.

Competing interests
No competing interests have been declared.

Citation
Douady S, Golé C. Fibonacci or quasi-symmetric phyllotaxis. Part II: botanical observations. Acta Soc Bot Pol. 2016;85(4):3534. https://doi.org/10.5586/asbp.3534

INVITED ORIGINAL RESEARCH PAPER

Fibonacci or quasi-symmetric phyllotaxis. Part II: botanical observations

Stéphane Douady[1]*, Christophe Golé[2]

[1] UMR 7057 Université Paris Diderot – CNRS, Bâtiment Condorcet, CC 7057, 10 rue Alice Domon et Léonie Duquet, 75013 Paris, France
[2] Department of Mathematics, Smith College, Northampton, MA 01063, USA

* Corresponding author. Email: stephane.douady@univ-paris-diderot.fr

Abstract
Historically, the study of phyllotaxis was greatly helped by the simple description of botanical patterns by only two integer numbers, namely the number of helices (parastichies) in each direction tiling the plant stem. The use of parastichy numbers reduced the complexity of the study and created a proliferation of generalizations, among others the simple geometric model of lattices. Unfortunately, these simple descriptive method runs into difficulties when dealing with patterns presenting transitions or irregularities. Here, we propose several ways of addressing the imperfections of botanical reality. Using ontogenetic analysis, which follows the step-by-step genesis of the pattern, and crystallographic analysis, which reveal irregularity in its details, we show how to derive more information from a real botanical sample, in particular, about its irregularities and transitions. We present several examples, from the first explicit visualization of a normal Fibonacci parastichy number increase, to more exotic ones, including the quasi-symmetric patterns detected in simulations. We compare these observations qualitatively with the result of the disk-packing model, presenting evidence for the relevance of the model.

Keywords
phyllotaxis; Fibonacci; quasi-symmetry; disc-stacking model; irregular pattern

Introduction

In the first part of this study [1], we used a disk-stacking iterative model on the cylinder to reproduce the successive appearances of primordia in phyllotactic patterns. This model assumes, in its very geometric nature, that a new primordium position is determined locally by only two older ones. As a result of the local determination of positions, irregularities of the initial condition do not get resorbed easily, and some never at all. Irregularity inevitably occurs when, as the disk size changes, the pattern undergoes transitions.

If the irregularities are small, and the speed of variation of the relative size of the primordia to the circumference slow, one obtains a normal Fibonacci pattern, with the numbers of helices in the pattern successors in the Fibonacci sequence. If the speed of decrease is too large and/or the irregularity too large, one tends to obtain a quasi-symmetric pattern, where the parastichy numbers are closer to one another (such as $(n, n+2)$, $(n, n-1)$, or even (n, n)). To our knowledge, these quasi-symmetric patterns, as a whole, were never explicitly mentioned in the literature before.

In this second paper, we provide evidence that the phenomena observed in the model's simulations do indeed occur in nature. Not only do we present regular plant patterns that exhibit the monotone Fibonacci transitions common in the model, and

irregular quasi-symmetric plant patterns from irregular initial conditions or fast transient, but we show, building on the work of Hotton et al. [2] in our plant pattern analyses, markers of the local, iterative nature of the pattern formation process.

To do so, we have to look carefully at the actual phyllotactic patterns. The descriptions of phyllotactic patterns are often reduced to the measurements of few numbers, as the parastichy numbers [3], or even only one, the divergence angle between two successive elements, often assumed to be essentially constant. Recent work [4,5] has tackled the large fluctuations in divergence angles often observed in plants, explaining them as switches in the order of onset of the primordia. Larger irregularity makes the divergence angle sequence look random however [6]. This is because it implies local changes of parastichy numbers. Such local changes were highlighted by Zagórska-Marek, who pointed out similarities with dislocations in crystals [7]. However, not many attempts followed to quantify such large irregularities.

We find these classical tools (parastichy numbers, divergence angle or its deviation from the golden angle) too focused on global aspects of idealized patterns, and thus inadequate to fully analyze patterns in transitions and with irregularities. In this paper, in order to perform the analyses of the plant patterns in the details needed to account for the local nature of the process, we develop the method used in [2] (ontogenetic graph) and introduce a new one (crystallographic graph). These graph concepts, that encapsulate all the local contact parastichies and their transitions, arise naturally from the disk-stacking model, as they consign the topological information of the disk contacts (ontological graph) or of the contacts of the Voronoï cells corresponding to the disk centers.

In plant patterns, these concepts translate into graphs that account for the contacts between the botanical elements (scales, seeds, leaf domains) constituting the pattern. Our focus on contacts, and not distance, enables us to consider mature plant samples, as we make the reasonable assumption that the contacts of mature organs reflect those in their juvenile state. The ontogenetic graph as applied to plant patterns, while it contains the information about the usual set of two parastichies, is a little subjective, especially at transitions, as it relies on determining which contacts are the two relevant ones. The crystallographic graph, on the other hand, keeps all the contact information, and reveals a third, secondary parastichy. From all the observations made possible with these tools, and the many cases observed, we then have a good, topological, evaluation for the botanical reality, and compare it with the model, either in detail as for the artichoke and birch catkin, or more loosely as with the graphs from our manual analysis of other patterns.

In Part I [1], our fundamental concept was that of fronts [2,8]. These are zigzagging lines of primordia in contact, encircling the stem. A front contains, at a given time of the pattern's evolution, all the primordia necessary and sufficient to determine the position of the next one. Fronts are subsets of the ontogenetic graph, and in turn the graph can be reconstructed iteratively from the fronts. Several fine measures can be made on fronts (see Part I), such as local parastichy numbers, resultant, front-averaged divergence and more. The irregularity of a pattern was also measured at the front level in Part I, as a combination of the deviations from their means of the "zigs" and the "zags". Because this measure of irregularity is based on lengths and distances, one runs into difficulties when adapting it to pictures of grown botanical samples. Indeed, secondary growth deforms the relative distances between the botanical elements. To come back to the front at its juvenile state, when its geometry (and its irregularity) determined the subsequent pattern formation one has to reverse engineer the supposed anisotropic growth. While it is possible to approximate such a process, it remains tied to uncertainties and subjectivity difficult to control.

Instead of pursuing the route of a numerical measure of irregularity in this article, we focus on topological markers of irregularity, that we discovered both by observing plants and by comparing disk-stacking simulations of regular and irregular patterns. These markers concern the types and respective locations of transitions in both the ontogenetic and crystallographic graphs.

One of the findings of this article is that irregularity is prevalent in plants. And while little irregularity coexists nicely with the usual Fibonacci transitions, our analyses of plant samples show that indeed irregularity drives the drift toward quasi-symmetry. Moreover the persistence of irregularity along a pattern, and the recognizable

topological markers it induces may be a sign of the relevance of the hard disk iterative stacking paradigm versus a more global, softer element paradigm in the determination of the pattern. In a further article, we will look more globally at the various types of patterns observed and the botanical conditions that may explain their genesis.

This paper is organized as follows: after the "Material and methods", we first introduce the concepts of ontogenetic and crystallographic graphs. We then use these tools to analyze a series of samples, each one showing different qualitative aspects, many of which were detected in the disk-stacking simulations of Part I. We start with a cabbage stem (monotone increase of Fibonacci parastichy numbers), continue with an artichoke flower bud (monotone decrease of Fibonacci numbers) and birch catkin (rhombic tiling). We then perform analyses of increasingly irregular *Pinus* female cones (regular Fibonacci patterns and irregular patterns in the same species). The *Cedrus* male cone shows a remarkable example of a drift from Fibonacci to quasi-symmetric, as predicted in Part I and a peteh inflorescence shows a solidly quasi-symmetric pattern, originated from a rapid transition. Next, we discuss the relation of these observations with the model of Part I. Finally we conclude, with some appendices and supplementary information.

Material and methods

Material

Pinus nigra femalle cones and *Cedrus libani* male cones were collected at Parc Montsouris, Paris, France (48.82186 N, 2.339 E). More irregular *Pinus nigra* female cones were collected at the pine "9", near Forêt Domaniale Notre Dame de Parlatges, on the side of D25 road (43.7824 N, 3.41329 E). For the pine cones, care was taken to humidify them in order to close them again in the position they had during their development, before imprinting (or unrolling) them. Looking at the detailed pattern of the scales, one can check that the expansion of the scales during their second spring does not change the contacts, as for turtle shells.

The decorative cabbage was bought in a Paris flower shop. The picture of the artichoke inflorescence come from [2]. The birch catkin from Harvard Forest, MA. The peteh *Parkia speciosa* inflorescence, with pods and beans, were bought in Bogor Market (Indonesia), in front of the Botanical Garden (6.60272 S, 106.80029 E) .

Plasticine (or modelling clay) imprinting

This method of imprinting consists in rolling the stem on a flat layer of plasticine. Rolling it with the right amount of oblique force allows the stem to roll while imprinting the plasticine. Then put a tangential light to reveal the relief in a photography. To have a good perception of the volume of the stem (and not its reverse) from the imprint, the best is to put the light in the lower position (or to put the light in the upper position, and inverse the picture). This technique works well for nearly cylindrical stems, with developed enough surface corrugation, to leave an imprint, but not too much, in order not to tear out the plasticine when rolling out. It can work even for not too cylindrical stems, such as conical slightly deformed pinecones. One problem is to maintain a constant force so that some parts are not unrolled more quickly, or leaving fewer imprints.

Mechanical unrolling

Mechanical unrolling used in this work consists to separate, in the spring, the still fresh and soft sapwood from the older hard wood. In the case of a pine branch, one can simmer for few days the removed part in essence, for instance turpentine. Once the sap is dissolved, one can remove the sapwood from the bark, containing the trace

of the leaf domains, and put it to dry flat. One can cut the sapwood and bark along a line parallel to the stem axis, and perpendicular, or along the contact parastichies themselves. The problematic point is to keep a record of the connection between the two unrolled sides, so that the periodicity is well kept. This work well for regular cylindrical stems. See supplementary material for an example.

Video unrolling

Video unrolling consists, for this work, in rotating regularly a stem in front of a camera. For this, a slowly rotating plate, with a motor, is best. The resulting movie can be imported in ImageJ, which opens it as a "stack" (pile of pictures). This pile of pictures can be interpreted as a 3D scan, and "resliced". If resliced along the axis of the stem, and the resulting picture taken around the image of the axis is chosen, this gives an unrolled projection of the surface. To reduce the time computation and searching for the correct middle picture, one can first crop the movie to around the stem axis, before reslicing. In the absence of a motor, one can take several side pictures of the stem, and them glue them together using anti-deformation computations, as is done for the reconstruction of panoramic pictures.

This works well even for not perfectly cylindrical stems and independently of the surface indentation (as long as there is a visual clue of the pattern). However, one then observes some local dilations/contractions of the surface, since being closer/further away from the rotation axis gives a slower/quicker rotation, and consequently an image that is (locally) enlarged/compressed in the horizontal direction. Ultimately these local deformations could be corrected. But in any case this optical projection preserves the original topology of contacts. One advantage is also that it produces a picture over more than a circumference period, allowing one to be sure of the period identification, and to choose the phase for the best drawing.

How to read phyllotactic patterns

Phyllotaxis patterns, from infancy to maturity

For our analysis of mature phyllotactic patterns, we make the following assumptions:

- At their microscopic onset, primordia are roughly circular, and of roughly the same size.
- Each new primordium is in contact with two older "parent" primordia on opposite sides of it. Exceptionally, a primordium can have three parents.
- Primordia first expand at a uniform rate to fill in the space left between them, forming polygonal units, whose edges mark the contacts between future organs.
- The polygonal units expand into leaf domains, scales or seeds as the plant grows. These grown and deformed polygons retain the contacts they had at their onset [9].

All these assumptions have to be taken with a grain of salt, of course. Primordia may have an elongated shape closer to ellipses, for instance. And the polygonal units they grow into might have edges that are not quite perfectly straight. The intuitive fact that contacts of polygonal units (leaf domains, etc.) remain during growth, probably helped by the rigidity of plant cell walls, would have to be substantiated experimentally [10]. This was shown in the case of *Magnolia* by Zagórska-Marek [11]. This being given, the phenomena we observe are qualitatively robust under deformation: they pertain more to the topology (with its notions of neighborhood and connectedness) of the pattern than to its geometry (which relies on distances). For this reason, we base our analysis of adult phyllotactic patterns on contacts of botanical elements.

Crystallographic and ontogenetic graphs

Our assumption of uniform rate of expansion of primordia means that a polygon's edge forms midway between the primordia it separates. If the primordia are perfectly circular and of equal size, the polygons can then be described as the Voronoï cells of the primordia centers: each cell contains exactly one center, and each point in the cell is closer to that center than to any other one (Fig. 1). It is a known fact that Voronoï cells of any set of points in the plane have in average six edges (see supplementary material).

Because of the extra regularity of the phyllotactic pattern, originating from the stacking of similar size primordia, most of the Voronoï cells associated to the primordia are indeed hexagons, with the rarer "defects" consisting mostly of pentagons and heptagons. The pairs of linked hepta and penta cells become prominent actors in the crystallographic pattern transitions [12,13].

In general, three edges of the Voronoï cells meet together. Only exceptionally one could have a meeting of four edges, or locally a square contact. But a careful examination then often allows decomposing a degree 4 connection into two very close Degree 3 connections. There is exceptionally even Degree 5 connections that are visible on real pinecones, as in Fig. 7. One can marvel at this exceptionally rare case (as we do in this figure), or decompose it into three close Degree 3 connections, which is easily done when zooming in.

We can connect the centers of adjacent cells by line segments. We obtain a planar graph (a set of points and non intersecting edges connecting them) called the Delaunay triangulation, because the regions that its edges bound are all triangles (with the above assumption of only Degree 3 vertex in the Voronoï graph). In our context, we can think of the edges of the Delaunay triangulation as "local" contact parastichies. We call the collection of primordia centers and local parastichies connecting them the crystallographic graph.

The regularity of the pattern implies that opposite sides of the hexagonal Voronoï cells are roughly parallel, and consequently, the Delaunay edges crossing these opposite sides are roughly aligned. Through each center of hexagonal Voronoï cell, then, there passes three pairs of these roughly aligned Delaunay edges. By extension, in a region where all the Voronoï cells are hexagonal, we can draw three sets of piecewise linear curves in three distinct directions. These curves are the contact parastichies.

In a phyllotactic pattern formed by circular primordia, with the assumption that each primordium is tangent to two older ones, two pairs of contact parastichies correspond to contacts of the circular primordia themselves. In the third direction, the primordia generally do not touch. We call the two pairs corresponding to primordia contacts the main local contact parastichies and the third pair the secondary local contact parastichy. In a regular pattern of circular primordia of equal size, the main parastichies connect nearest neighbor primordia and the secondary local parastichy corresponds to the two smaller sides of the Voronoï cell.

We call the graph formed by the primordia centers and the main local contact parastichies the ontogenetic graph. Hence, the ontogenetic graph connects each primordium to its parents (and not more). The ontogenetic graph is thus obtained from the crystallographic graph by removing the secondary contact parastichies. In a region of the pattern where the pattern sees no transition, the ontogenetic graph consists of the two families of parastichies one perceives the most, and that are counted to classify the pattern.

The notions we've introduced in the context of perfectly circular primordia of equal size can generalize to more realistic situations where primordia are not quite circular, and not of equal size. The Voronoï cells are further deformed during secondary growth into leaf domains, seeds or scales. We will call these generalized Voronoï cells. Because of our assumptions in section "Phyllotaxis patterns, from infancy to maturity", the topologies of the crystallographic and ontogenetic graphs remain unchanged by these deformations as they are based on the contacts of botanical elements. We will see that, even though the ontogenetic graph is a subgraph of the crystallographic one, the two graphs provide complementary information about a pattern's transitions and regularity.

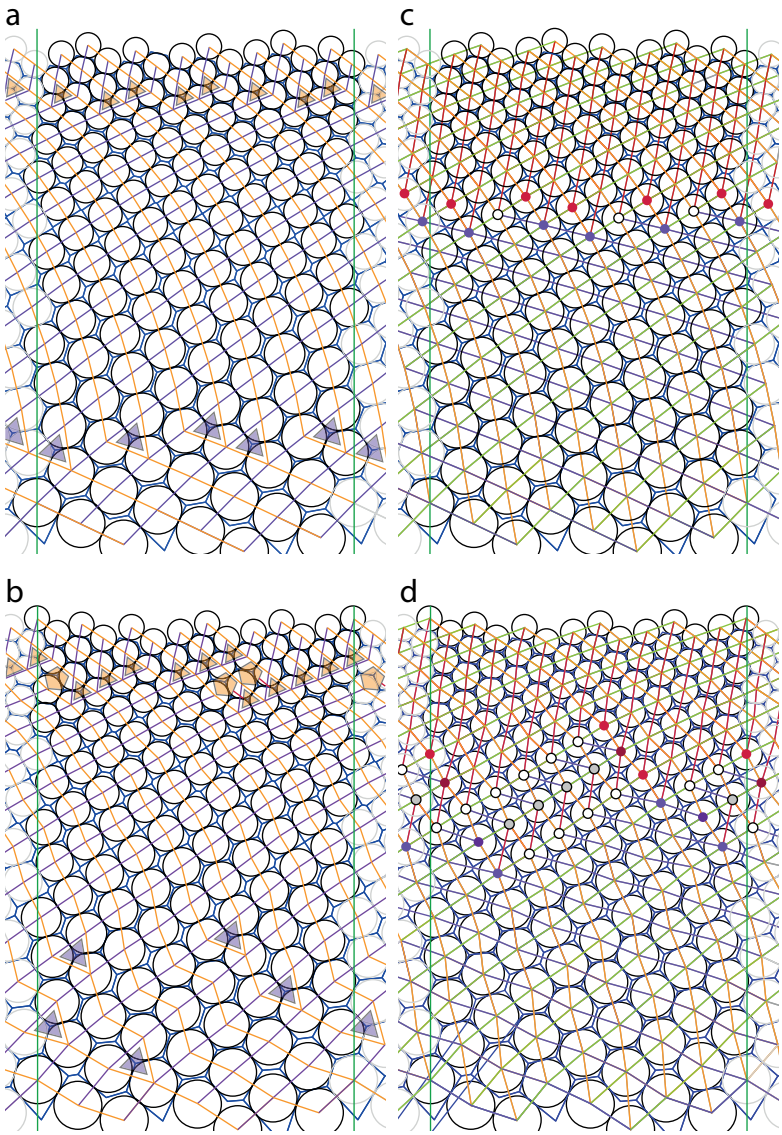

Fig. 1 Ontogenetic and crystallographic analyses of regular and irregular patterns. The green vertical lines show a period of the cylindrical patterns. The patterns show continuous transitions from (3, 5) to (8, 13) obtained from disk-stacking simulations as in Part I, with identical decrease of relative primordia size with height. **a** and **c** show the analyses of the same, very regular pattern, starting with a front of three identical up vectors and five identical down vectors. **b** and **d** analyze the same, more irregular pattern, with fluctuations in the initial front vectors (visible by their wiggling). We used a computer program to draw the Voronoï cells associated to the disk centers (polygons in thin, blue). They approximate the generalized Voronoï cells that would more neatly enclose the disks of varying size – but without change of topology. **a,b** Ontogenetic analysis of the patterns. Main parastichies are colored according to whether they connect a primordium (disk) to a left or right parent. Transitions in the graph take the form of triangular, or pentagonal faces instead of the more common rhomboidal ones. When this happens, one of the main parastichies is replaced by the secondary one, and vice versa. These transitions appear around the hexagonal stacking region. In the irregular case (**b**), one can see a larger spread of the transition zone. Surprisingly, some parastichies present no bifurcations. Note also the occurrence of adjacent pentagon-triangle pairs in that case. **c,d** Crystallographic analysis of the same patterns as in **a** and **b**. Centers of Voronoï cells which are in contact with one another are connected by a line segment. As the average number of contacts is 6, three parastichies usually cross at each point. The parastichies segments are colored according to their orientation. New secondary parastichies start and old ones stop at Voronoï cells that are close to squares, as contacts appear and disappear there. This is also where the ontogenetic graph presents rhomboid that are closest to square, and thus farthest away from the transitions in the ontogenetic graph. As one goes up the regular pattern, the more horizontal secondary parastichies (in blue) terminate and the more vertical one (in red) start. In the irregular pattern, there can also be switchbacks, with the more vertical parastichy stopping after a short segment, and the more horizontal one starting anew, also for a short segment. The starting point of a red (more vertical) secondary parastichy is colored in red if it does not belong to the blue secondary parastichy. The Voronoï cell is then a pentagon. If the starting point is inside the blue (more horizontal) secondary parastichy, it is colored blue. The Voronoï cell is a heptagon in this case. If the starting point of a red secondary parastichy is also the endpoint of a blue one, it is colored white. At such a point, the Voronoï cell is a hexagon, but with its short sides not opposite. The switchback points of the irregular pattern, where the blue (more horizontal) secondary parastichy starts again are colored gray if a red parastichy ends there (hexagonal Voronoï cell), and dark blue/dark red otherwise (pentagonal/heptagonal Voronoï cell). Note the alignment of these gray and dark points along a main parastichy.

Pattern transitions and the graphs

The ontogenetic graph is directly tied to the dynamics of the pattern formation, as modeled in Part I [1]. We described these transitions in terms of front, the latest layer of primordia formed in the peripheral zone of the meristem at a given time. From a vertex in the ontogenetic graph, one can build a front by connecting the vertex to its right parent, and then proceeding to the right through local parastichies, trying at each step to stay as high as possible without going higher than the original vertex. The process stops when, having gone around the cylinder, one reaches the original vertex. When the pattern is regular, its parastichy numbers can be read off as the numbers of up and down vectors in the zigzagging front. When a new primordium is added on top of the front, there is no change of parastichy numbers as long as its parents are separated by exactly one other vertex in the front: to obtain the new front, a pair of down and up vectors were changed into a new pair of up and down vectors, keeping the front parastichy numbers the same. Changes occur when the parents are adjacent in the front (triangular transition) – in which case their is a net increase of 1 in one of the parastichy numbers, or if the parents are separated by two other front vertices (pentagonal transition) – in which case there is a decrease of one of the parastichy numbers by 1. Higher polygon transitions can also occur, but are much rarer. Triangular transitions happen when the front vectors are close to 120°. In terms of disk-packing, this corresponds to the region of a pattern where the packing is close to hexagonal, and the Voronoï cells are close to being regular hexagons.

Transitions in the crystallographic graph take a different form, and interestingly are located in different regions of the pattern. They correspond to a change in the number and kind of contacts, i.e., in the number of sides of the (generalized) Voronoï cells, as well as the orientation of the cells in contact. They happen in regions where two sides of the Voronoï cells are small and the faces of the ontogenetic graph are close to being square. In other words, as far away as possible from the transitions in the ontogenetic graph. The Voronoï cell at a transition is usually either a pentagon or a heptagon, or a hexagon with its short sides not opposite.

In terms of parastichies, transitions in the ontogenetic graph occur when the secondary parastichy and one of the main ones exchange roles. In terms of the main parastichies, one stops when there is a pentagon transition, one is created when there is a triangle one. In a crystallographic graph transition, a secondary parastichy terminates and/or another one begins.

Detecting irregularity. An important aspect of this work is the study of the role of irregularity in the creation of Fibonacci-like or quasi-symmetric patterns. In Part I [1], we measured irregularity by combining the deviations from their means of the up and down vectors of fronts. The front of the (same) pattern shown in Fig. 1a,c has irregularity 0: its three up vectors are the same, and the five down vectors are the same, and thus their is no deviation from the mean. Fig. 1b,d show a pattern that is more irregular: the up vectors are not all the same, and neither are the down vectors. Their deviation from the mean, and thus the irregularity of the front, is not 0. As shown in these simulations, irregularities propagate along the pattern. To use this kind of front-based measure of irregularity in botanical samples, one has to first carefully correct the deformations due to the data collection method, and the non-uniformity of the overall geometry of the sample.

But, Fig. 1 gives some keys for visualizing irregularity without measuring it on fronts. In the figure, the irregular pattern show more scattered transition sites, both in the ontogenetic and crystallographic graphs. More importantly, the crystallographic analysis shows types of transitions (switchbacks) in the irregular patterns that regular patterns do not have. These can be seen as topological markers of irregularity based on contacts which therefore (given our assumptions) reflect the irregularity of the pattern at its birth.

Comparing ontogenetic and crystallographic analyses of botanical samples. While the ontogenetic graph gives the most commonly sought features of a pattern, namely, its main parastichies and their numbers, it is difficult to pinpoint exactly and objectively the locus of transitions in a pattern. Indeed, since transitions occur when a secondary parastichy becomes primary and vice versa, they can only be objectively

located by detecting equal sides in the Voronoï cell. In an adult pattern, where distances have been deformed this is clearly full of uncertainty. One could deform back the pattern till it fits better a disk-stacking pattern. But the expansion of the stem, which needs to be reversed, is often non homogeneous. The pairs of pentagon/triangle transitions are also often hard to distinguish from pairs of quadrilateral transitions. However, in practice, the fluctuation in the location of the transitions due to these uncertainty is relatively small, and the qualitative, topological information remains roughly unchanged.

The crystallographic transitions are more objectively detected, as they often occur in generalized Voronoï cells where a change in the number of adjacent cells is not 6. "No contact" being easier to detect than "equal contact", these transitions are easier to pinpoint precisely and objectively. Moreover, in more irregular patterns, the transitions are more spread out and certain transitions (switchbacks) only appear in irregular patterns. This is a real advantage when one wants to get a qualitative sense of the irregularity of the pattern. On the other hand these transitions are not where the ontogenetic graph is changing, with the associated changes in parastichy numbers. In regular patterns, this is also where the divergence angle, which changes monotonically while the parastichy pair of numbers is constant, is switching from increasing to decreasing, or vice versa [14–17]. The two analyses thus highlight transition places that are dual from each other (see Fig. 1). However, since quadrilateral transitions propagates geometric features of the pattern along the parastichies, the imperfections present after an ontogenetic transition near an hexagonal state can propagate and be also visible in the crystallographic analysis around the square state. In this way they are not only complementary but also correlated.

In our graphical analyses, we color coded parastichy segments. Passing through a cell, one has to decide which pairs of local parastichies are in the same direction, and must be colored the same way. Similarly to grouping street segments between two crossings into large scale streets [18], one can look at the angles formed by the connection lines at the center of a cell, and group them in pairs by closest orientation. This can be a little tricky on very irregular patterns, such as Fig. 6 and even more Fig. 7. In the ontogenetic graph, we highlighted triangular and pentagon transitions with little iconic triangles and pentagons within those faces. In the crystallographic graphs, we marked the point where a parastichy starts or stops with the color of the parastichy. When both events happen at the same point, we marked it in white. In a pattern with decreasing primordia size, the set of secondary contact parastichies are globally replaced by a more vertical set. In more irregular patterns, the transitions can happen with switchbacks, where such transitions can be temporarily undone by reverse transitions (see Fig. 1). These switchbacks can then serve as objective markers of irregularity.

Botanical observations

The main question in Phyllotaxis is to determine the origin of the pattern observed. Since the early observation of Hofmeister [19], it is clear that the phyllotactic pattern is built step by step at the border of the apical meristem. To understand the evolution of a pattern one thus needs to retrace its successive modifications from a simple starting initial condition (as we have done in the model of Part I).

The first example we present is of the leaves around a cabbage stem, showing indeed the occurrence of increasing Fibonacci numbers of parastichies through a sequence of Fibonacci transitions starting from a (1, 1)-front as described in Part I. Strangely enough, while such transitions are widely assumed to be prevalent, explicit examples are rarely shown.

Patterns with decreasing Fibonacci numbers are more easily observed in Asteraceae inflorescence, with large parastichy numbers, or in pinecones, for smaller ones. We analyze a juvenile artichoke meristem [2], where the microscopic pattern has undergone very limited secondary growth and is thus only very slightly disturbed, and where the disk accretion model can be directly tested.

For another quantitative comparison of the disks accretion model with a real botanical pattern, we present the case of a birch catkin, where the elements and their contact is still visible and where the secondary growth effect can be easily reversed. This yield a rhombic tiling, as commonly encountered in the disk-stacking model.

Later we show examples of pinecones of the same species (*Pinus nigra*) but with widely varying regularity and patterns.

Finally we present the case of a *Cedrus libani* male cone, where we observe the convergence from an irregular Fibonacci pattern toward a quasi-symmetric one, and a peteh inflorescence stem, directly quasi-symmetric after a very short transient, as predicted by the model.

Increasing Fibonacci: the example of decorative cabbage stem

In Part I, we presented numerical evidence that, in the disk-packing model, if a pattern starts with a (1, 1) front that is not too flat and if the rate of decrease of the radius of the disks is slow enough, then the pattern must follow the "monotone golden ratio scenario" where only triangle transitions occur, one side at a time, yielding fronts of increasing Fibonacci parastichy numbers. The cabbage stem of Fig. 2 with its clearly visible leaf scars in compact stacking, presents an iconic example of this phenomenon. Yet, one can see that even in this nearly perfect scenario some trace of irregularity at the very top, where triangle transitions are not spread quite evenly among parasticies. That the scenario can survive, some irregularity is a sign of its robustness.

Decreasing Fibonacci: the example of artichoke composite flower

In the latest stages of morphogenesis, in its inflorescence, the meristem of an Asteraceae (e.g., daisy, sunflower, and artichoke here) fills in with primordia, of roughly the same size while the inflorescence size, in that time frame, remains close to constant (Fig. 3). In the previous study [2], we defined the ontogenetic graph for such patterns as the graph whose vertices are the centers of the primordia and edges connect each primordium to its parents. In that paper and algorithms used in it, we defined parents as the two closest primordia away from the center, and on opposite sides. While this is different from the contact-based definition of this paper, the two differ only slightly in the case of a regular pattern such as shown in Fig. 3, giving results of the same qualitative nature (the pentagons would be slightly shifted, but in same numbers. There can also be some pentagon/triangle pairs in one case that are not in the other).

Fronts were defined in that context as zigzagging curves going in one direction that try to be as close as possible to the center without being closer than the starting point – thought of as the state of the meristem edge at a given time of the morphogenesis. Parallelly, the paper [2] used a disk-stacking model on the disk to model plant inflorescence morphogenesis, where the role played by height in the cylinder is replaced by distance to the center of the disk. The ratio b of primordia size over the circumference of the shrinking meristem is then increasing, yielding mostly pentagonal transitions in the fronts.

Fig. 3 shows a striking example of a reverse golden ratio scenario: instead of fronts parastichy numbers increasing, one side at a time, via triangle transitions, they are now decreasing, one side at a time, via pentagon transitions. Except for the lonely triangle transition at the top, neutralized by an adjacent pentagon. Similarly to the cylinder case, red pentagons correspond to front transitions where, as one proceed toward the center, two red edges and a green one yield one red edge and a green one, and similarly for the green pentagons. One can count 35 red pentagons in the outer transition which, with one of them neutralized by the red triangle, yielding a net 34 pentagon transitions and a decrease of the number of red edges in the front from 55 to 21. The inner transition shows a clean set of 21 green pentagon transitions, decreasing the number of green edges in the front from 34 to 13. The lone triangle transitions is the only detail that keeps the pattern from following a (reverse) monotone golden ratio scenario.

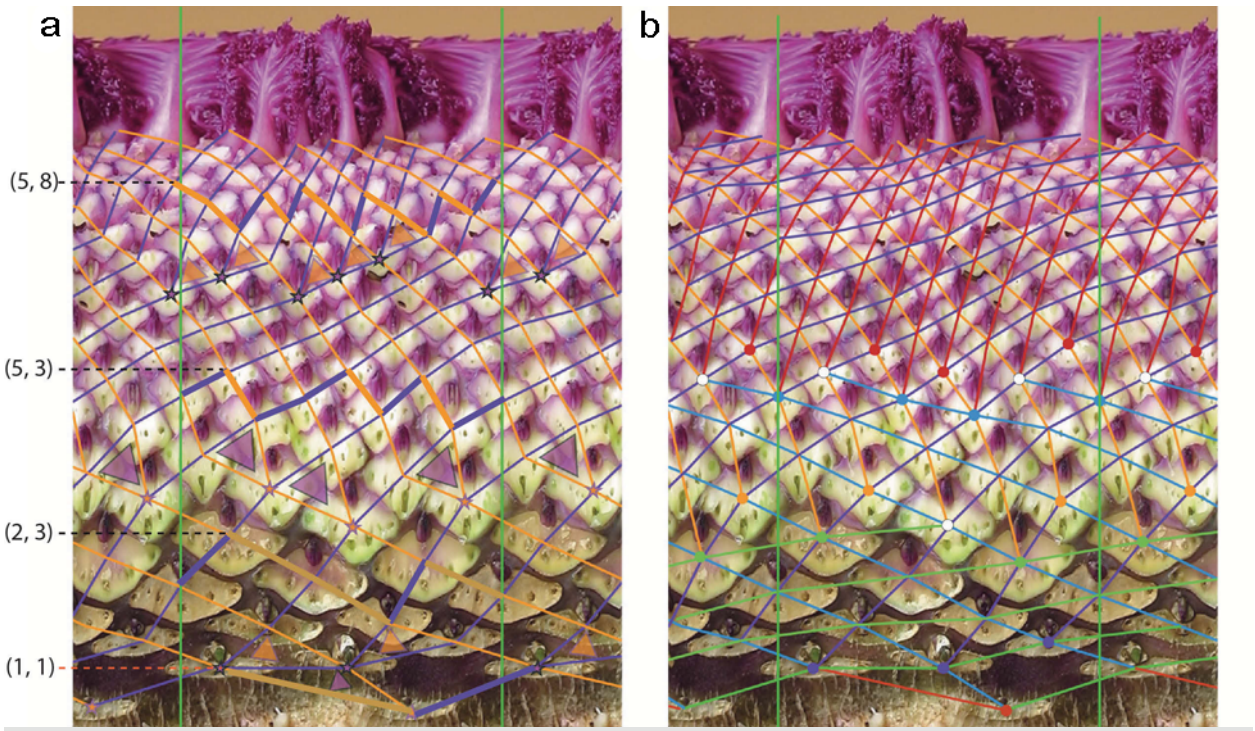

Fig. 2 Cabbage stem. **a** Decorative cabbage *Brassica oleracea* var. *acephala* vegetative stem unrolled by video. The green lines show a period of the cylindrical patterns. One can clearly see the leaf scars with their axillary buds, touching each other. Although cabbage is a dicotyledon, we see an isolated leaf scar at the base of the stem, creating a (1, 1) initial condition. The parastichy numbers then increase from (1, 1) to (5, 8). **a** Ontogenetic analysis. Fronts of increasing Fibonacci numbers are indicated ((2, 1) is left out for graphic clarity). Transitions are only triangular, consistent with the "monotone golden ratio scenario" of Part I. The last transition shows a hint of irregularity, as the triangles are more aligned along the bifurcating parastichy direction, leaving one parastichy untouched, as in Fig. 1b. **b** Crystallographic analysis. All the transitions fit those of a perfectly regular disk-stacking.

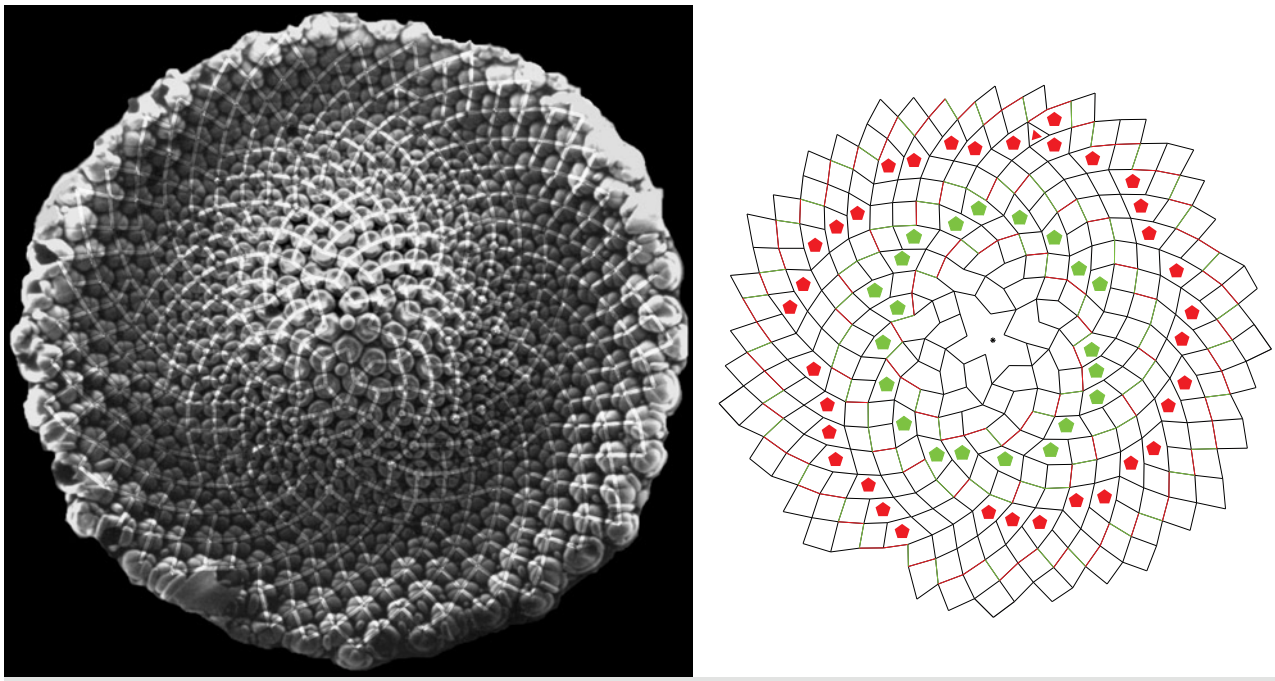

Fig. 3 Decreasing Fibonacci transitions in an artichoke inflorescence. From the electron micrograph of the meristem, positions of the center of each primordia were manually collected, as well as that of the meristem. As the primordia have nearly equal size, the ontogenetic graph was then built with a computer program using distances and the Delaunay triangulation, removing some edges. Its image is superimposed onto the micrograph, and shown again on the right. Another computer program determined the front at any chosen point that is reasonably away from the edges of the pattern. Three concentric fronts are shown on the right, with parastichy numbers (34, 55), (34, 21), and (13, 21), respectively. They are separated by two zones of pentagon transitions, all red first, then all green, according to which parastichy direction is involved. Only the red triangle transition at the top, neutralized by a red pentagon, makes this pattern not quite a perfect example of reverse monotone golden ratio scenario.

While the above analysis of the pattern was performed on the ontogenetic graph produced with the data, in [2], we showed that, using the disk accretion model, one obtains a pattern that is a good fit to the data, and the corresponding ontogenetic graph produces qualitatively the same transition patterns.

Rhombic tilling: the example of birch catkin

In Part I [1] (see also [8]) we introduced the concept of rhombic tiling. These can be seen as deformations of rhombic lattices, where the segments of lines of the lattice are allowed to deviate from perfect alignment. In the disk-stacking model on the cylinder, these patterns form attracting sets: a pattern close to a rhombic tiling converges to a close-by rhombic tiling, often in finite time. We claim here that rhombic tilings are a better model than lattices for plant patterns that show no transitions. Indeed, they not only account for the often visible undulations of parastichies, but also for difficulty to perceive shifts in the vertical order of primordia, which yield erratic divergence angles. Rhombic tilings, as opposed to lattices, can present some substantial irregularity. This irregularity never gets absorbed in subsequent iterations, and in fact stays constant: the pattern is periodic and all of its fronts are made of the same vectors.

Fig. 4 presents the analysis of a rolled out a birch catkin, collected at Harvard Forest, MA. In this regular looking sample, there are shifts of vertical order in the primordia that induce erratic divergence angle. While the lattice model cannot account for this phenomenon, it can be found in seemingly regular botanical patterns.

Regularity and irregularity in one species: the example of *Pinus nigra* female cones

Pinecones can present very different aspects, from very regular to very irregular [3]. Cones in some species, for instance in *Pinus pinaster*, also present a typical inversion of gravitropism, first pointing up and then pointing down, associated with an over expansion of one side. This asymmetric expansion is present but reduced in the case of *Pinus nigra*. Here we present the most regular female cone we found as well as two irregular non-Fibonacci cones harvested from a tree that had been pruned. This tree then presented a larger percentage of non-Fibonacci cones than observed in [3], as we will discuss in a future article.

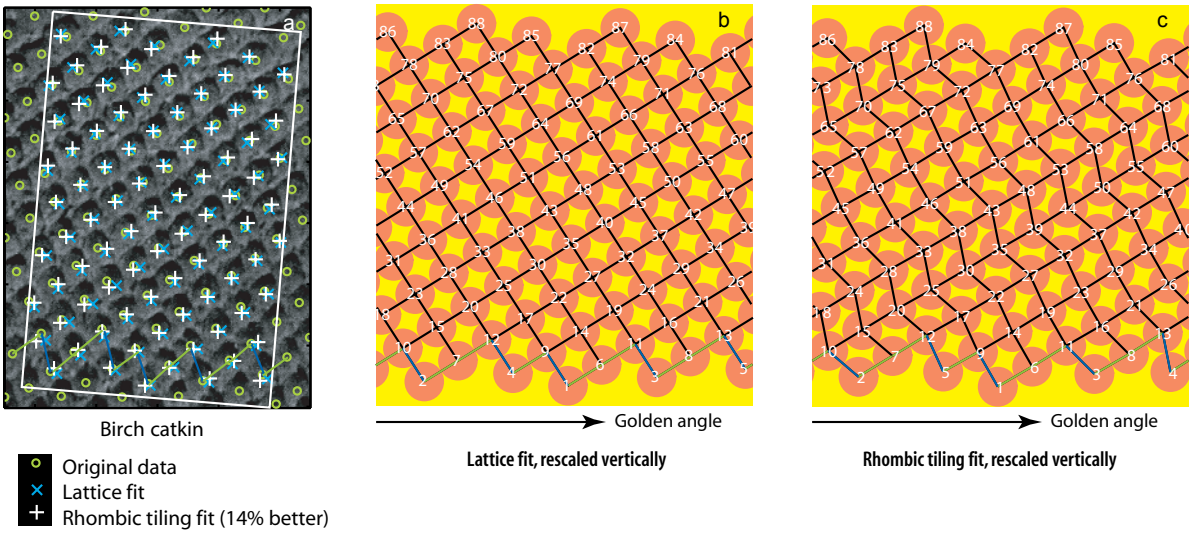

Fig. 4 Analysis of a birch catkin. **a** The imprint of a birch catkin rolled on clay. After a vertical compression counterbalancing anisotropic growth, we used a method of least squares with (nonlinear) constraints to fit lattices and rhombic tiling to this pattern. The results of this process are seen in the lattice in **b**, and the tiling in **c**. The fit for the rhombic tiling is 14% better than for the lattice. More importantly, the divergence angle between subsequent disks is very close to the golden angle in **b**, but it can vary dramatically in **c**, e.g., between the pairs of disks (5, 6) and (7, 8).

Despite its regularity, the crystallographic analysis (as well as the ontogenetic one) of the regular cone (see Fig. 5) reveals some trace of irregularity. But this irregularity is minor in comparison with those revealed by the analyses in the two non-Fibonacci cones from the pruned tree (Fig. 6, Fig. 7). The ontogenetic analysis can further give the whole sequence of unexpected transitions between patterns when the parastichy numbers reduce.

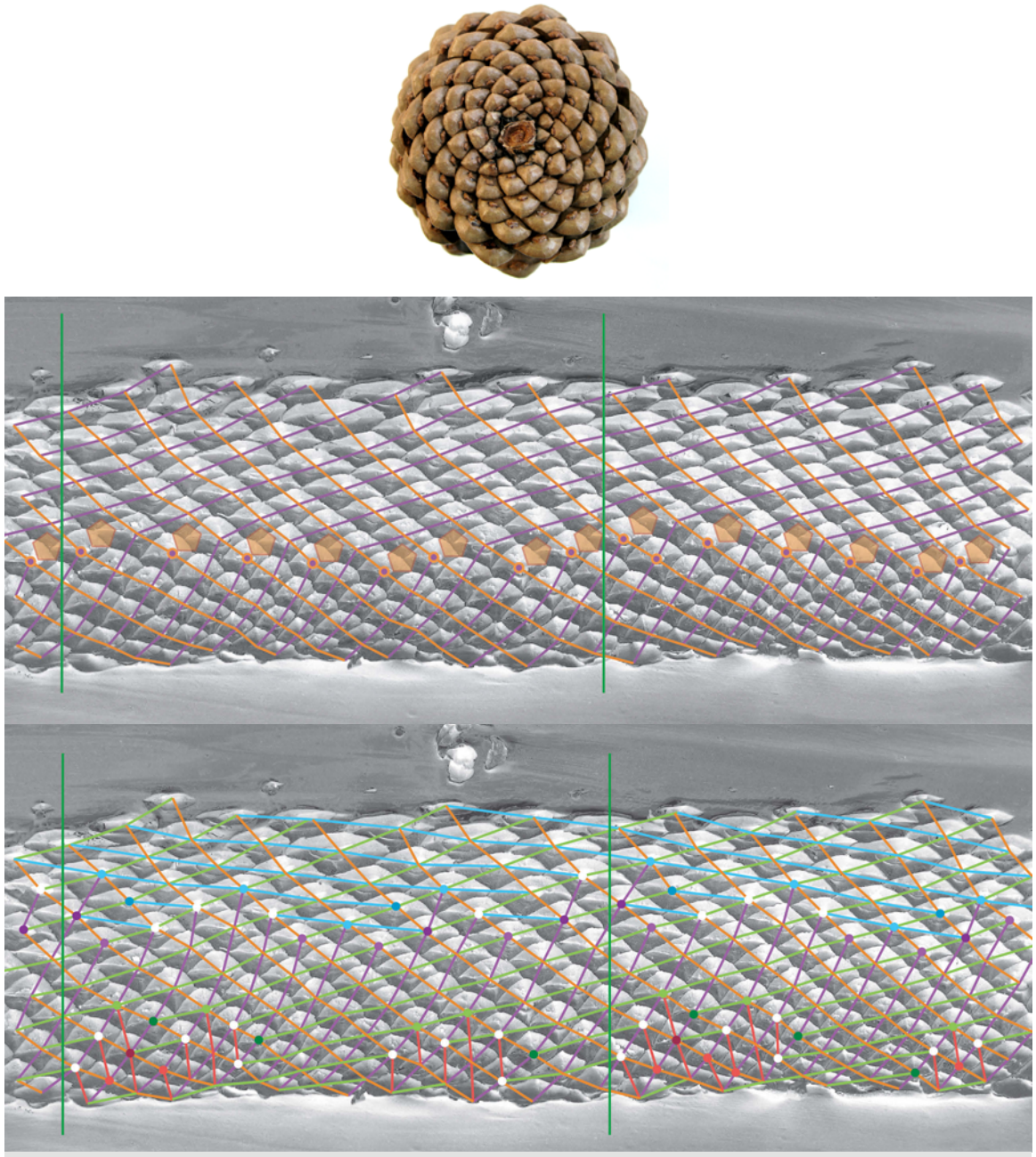

Fig. 5 Very regular *Pinus nigra* cone. This cone, collected in Parc Montsouris (Paris), presents the most regular pattern we have found. Top: bottom view of the cone, when dried-open. The square scales make the two opposite (13, 8) parastichies very visible. Middle: lateral imprint when humid-closed, with its ontogenetic analysis. The green vertical lines indicate one period of the cylindrical pattern. One can read a (13, 8) to (5, 8) transition, with the expected five pentagons. A hint of irregularity can be seen in their spreading, as there is one pair and a triplet of aligned pentagons, which are close to each other, while one would observe three pairs of aligned pentagons with one pair separated by isolated pentagons in a perfectly regular case, as in Fig. 1a . In this previous image, the Fibonacci numbers are increasing, so the transitions were triangles, while it is decreasing here, with pentagons. But the regularity – or not – of the transition points is identical. Bottom: the crystallographic analysis of the same imprint reveals that it is not perfectly regular, as the highest number parastichies (in red, lower portion) is observed on only parts of the circumference. The five green parastichies that remains there form stairs running along one direction, as in Fig. 1d.

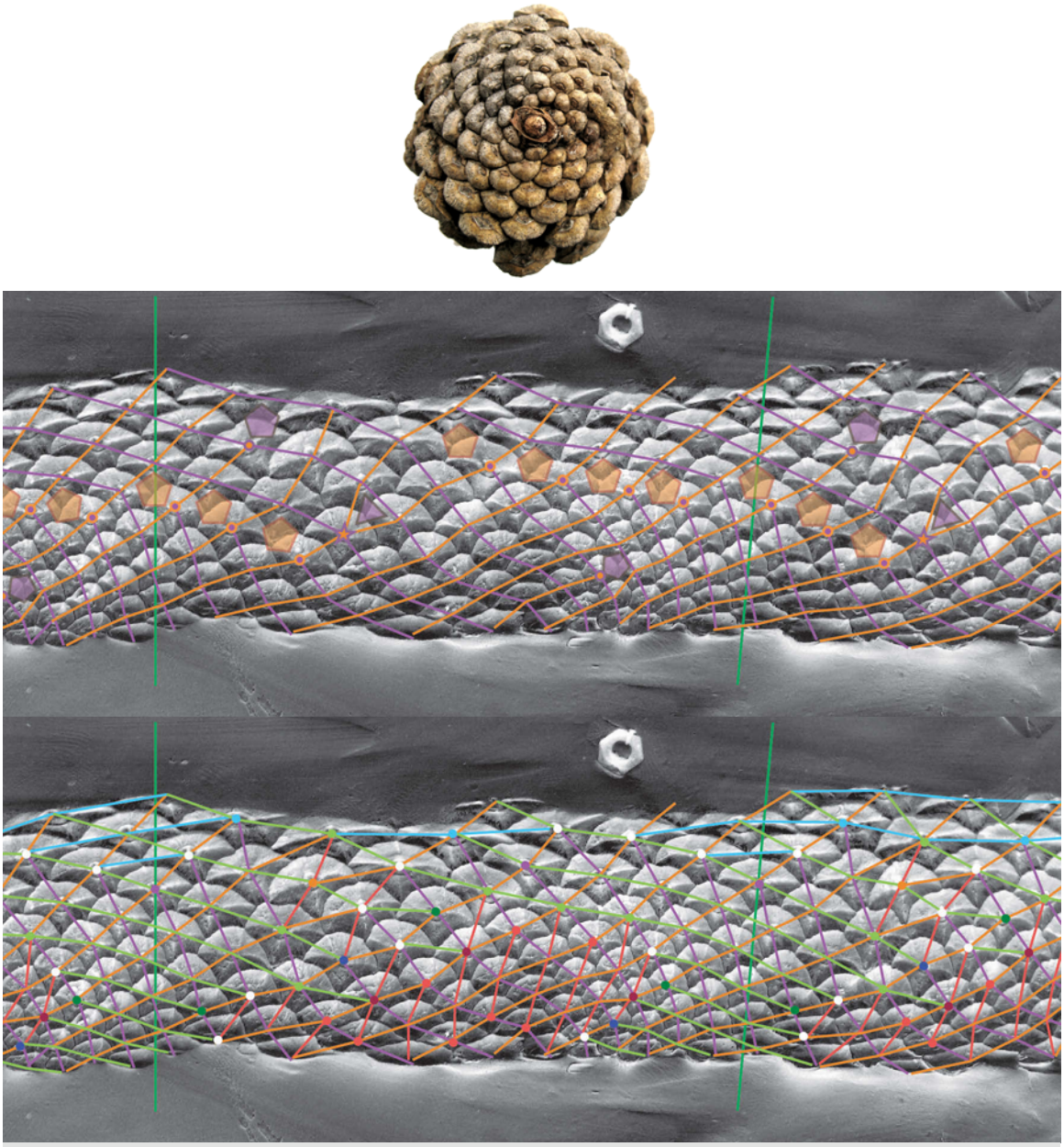

Fig. 6 An irregular *Pinus nigra* cone. One example of non-Fibonacci cone cropped from a pruned *Pinus nigra* tree (43.7824 N, 3.41329 E). Top: bottom view when dried-open. One can read off a (7, 11) (Lucas) pattern. Middle: the lateral imprint when humid-closed, with the ontogenetic analysis. One can see the irregularity and that the (7, 11) pattern at the bottom, presents an isolated pentagon leading to a (6, 11) pattern. The further very spread transition, with seven pentagons along the 11 direction very aligned, and a triangle in the opposite direction, lead to a (7, 4) pattern before an isolated pentagon leads to (6, 4). The first isolated pentagon-triangle could be grouped in a pair (and dismissed to yield an approximate reading of a plain (7, 11) to (7, 4) transition), but another sign of irregularity is that they are not aligned along the opposite parastichy direction. Bottom: same imprint with crystallographic analysis. The contact analysis is not sensitive to the visibly larger expansion on one side, making larger scales and expanding locally the pattern. One can see a very irregular system, with two pentagonal connections with exchange of parastichy colors, colored in dark blue.

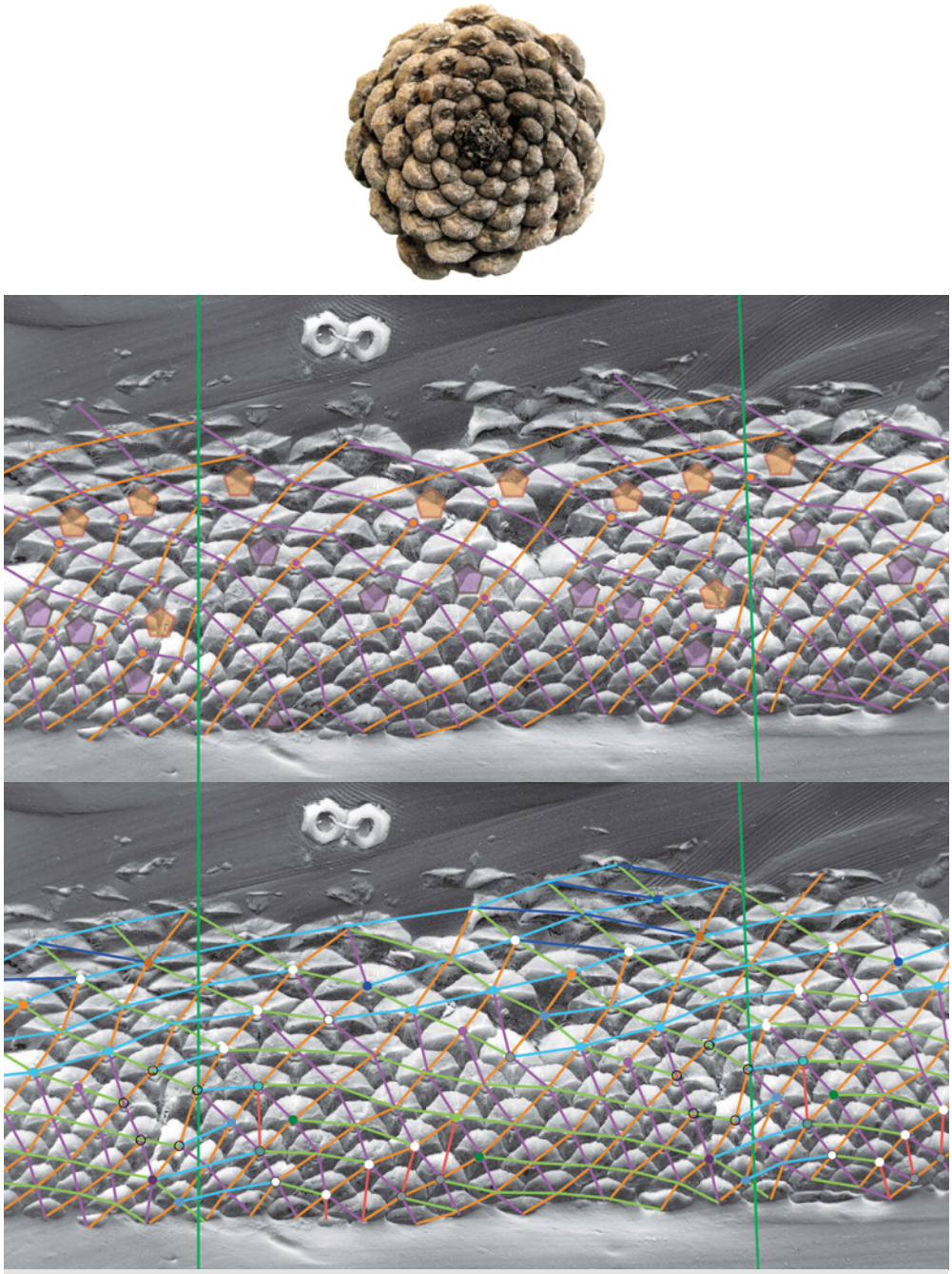

Fig. 7 A very irregular *Pinus nigra* cone. Another example of non-Fibonacci cone cropped from the same pruned tree of the previous figure. Top: bottom view when dried-open. One can read a (11, 9) pattern. Middle: the lateral imprint when humid-closed, with the ontogenetic analysis. One can see that the (9, 11) pattern at the bottom, transitions quickly to a (9, 10) pattern with an isolated pentagon. It is followed by a spread out series of five pentagon transitions in a direction and an isolated one in the other direction, leading to a surprising Fibonacci (8, 5) pattern, before a nearly regular five pentagon transition, if they were aligned, leading to the previous pattern in the Fibonacci sequence (3, 5). This ending in Fibonacci numbers could be interpreted as what the model predicts, the noisy Fibonacci turn quasi-symmetric, but reversed in variation of relative primordia diameter. Apart from this happy ending, one can see a very special region of vertically extended scales the lower isolated orange pentagon. Bottom: same imprint with crystallographic analysis. A rare connection between the scales, of Degree 5, have been surrounded by black circles, without trying to reduce it into Degree 3 connections. The very large irregularity makes the grouping in colors of the local connections particularly difficult, for instance between the purple and the green, or between the green and light blue even though they are of opposite chirality. This also leads to the presence of many exotic transition places, for instance surrounded by dashed circles. But even in this case the presence of higher order red parastiches at the bottom propagate regularly along the orange parastiches.

Drift toward quasi-symmetry in a *Cedrus libani* male cone

Cedrus libani has regular (3, 5) female cones (see supplementary material). However, the male cones, appearing also in the fall, rise to much larger parastichy numbers, here (13, 21) in apparently a very short number of primordia, before stabilizing and producing a large numbers of elements. While this still leads to a Fibonacci pattern at the base, the fronts at the base are very irregular, and this irregularity with a nearly constant relative primordia diameter makes the pattern converge toward a quasi-symmetric state, as detected and explained in Part I [1] with the disk-stacking model.

A direct quasi-symmetric state in peteh flower stems

The male cone of *Cedrus libani* shows a drift toward the quasi-symmetric state, even while starting from a Fibonacci front, and with little overall change in the ratio b of primordia diameter over circumference of the stem. This can be explained by the strong irregularity of the starting fronts. This irregularity comes in turn from a very quick transition to relatively high parastichy numbers that preceded these fronts. Indeed, Fig. 5 in Part I [1] shows that for a too rapid a decrease of relative primordia size, the pattern tends to quickly become a quasi-symmetric state (see also how that happens in Fig. 13 of that paper). Here in the case of the peteh (*Parkia speciosa*) inflorescence stem (Fig. 9), one can see that from few involucral bracts, the inflorescence transits very quickly, apparently instantaneously, to a large number of very small flowers. We then observe a quasi-symmetric state ((21, 22) in this specimen), as predicted by the model in Part I.

Discussion

Origin of parastichy numbers

Most of historical phyllotactic observations in the literature are done on mature organs and on these organs only part of the ontogenetic process is visible. More recent observations of the meristem is often limited to one or few successive snapshots, and never to a full recording of the ontogeny. Only in a few cases, such as the mature sunflower stem can one see the trace of the first primordia (in this case a pair of cotyledons), and how the pattern emerged from them [20]. Such rare examples are also usually limited to small final parastichy numbers, such as (2, 3). For higher numbers, for instance on the pinecones, one can barely see the phyllotaxis of the base stem that supports it, and even less how the phyllotaxis of this side stem originated. To know the origin of parastichy numbers one needs to see their successive transitions.

This makes our example of cabbage precious in that it helps visualize Fibonacci transitions from the start to a relatively large (5, 8) structure. It confirms the viability of the golden ratio scenario, and helps extrapolate its applicability to other plants.

Assuming such an orderly scenario, with, e.g., Fibonacci-like transitions, for the occurrence of the more exotic parastichy numbers is much more problematic. And the more distant from Fibonacci parastichy numbers, the quasi-symmetric states for instance, the more problematic it becomes to deduce the starting point and past evolution of a pattern, especially if nothing is known of the early part of the pattern.

For instance, the (7, 12) pattern observed on a pine branch (see supplementary material), could come from (7, 5) and then previously (2, 5). However, as already noticed by Zagórska-Marek [7], such pattern rather appears through a minimal number of localized bifurcations from a normal Fibonacci pattern, or already a quasi-symmetric one. For instance, it could also come from a (8, 13) Fibonacci pattern, with just one pentagon/triangle for each direction.

Such simple transitions, with a logic in their disorder, are precisely what we observed in detail in the male cedar cone (Fig. 8). Whereas reconstructing the finally observed (16, 14) pattern assuming pure Fibonacci transitions would impose to

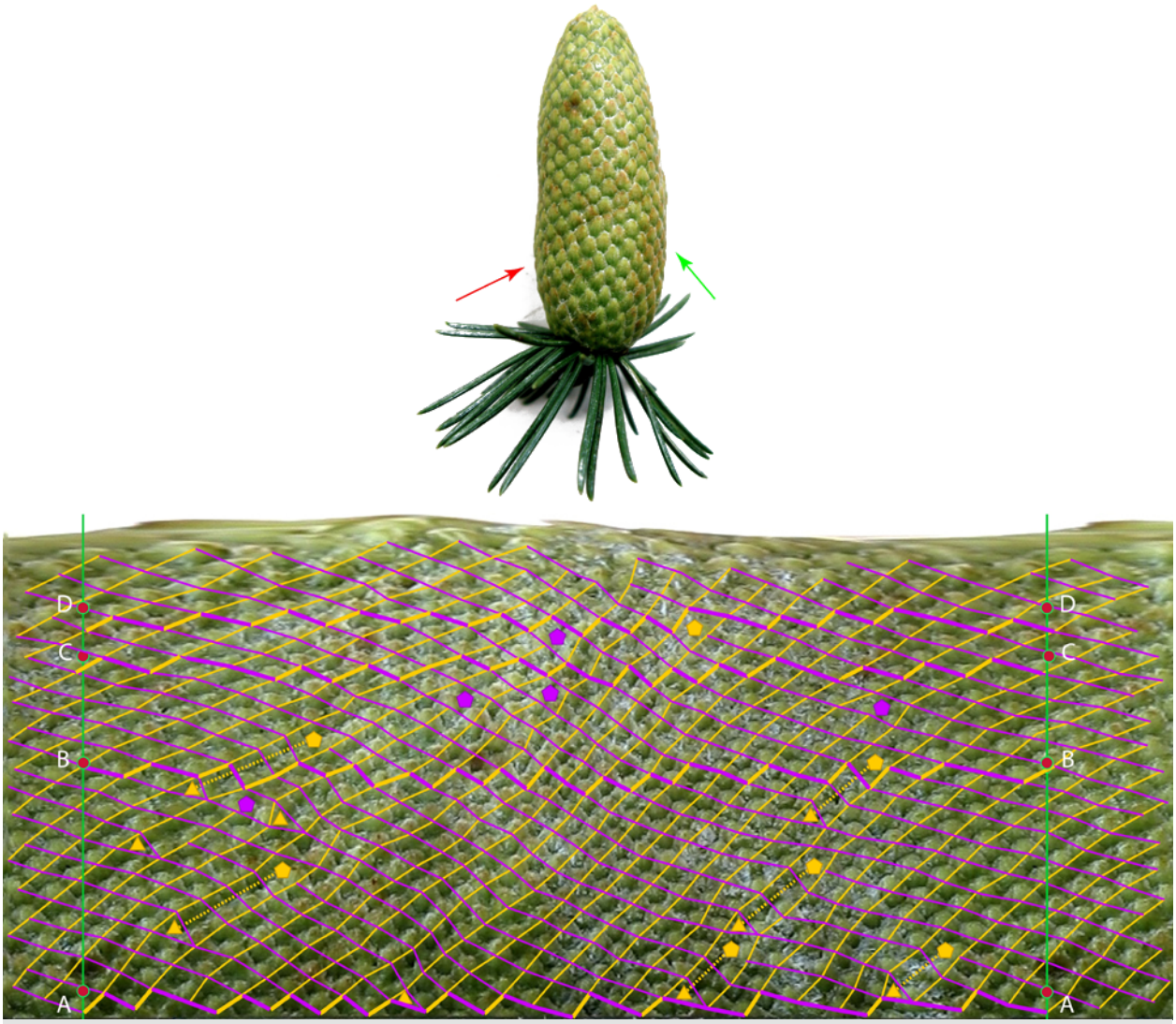

Fig. 8 *Cedrus libani* male cones (from Parc Montsouris, Paris). Top: side view of a cone. On can see two lines of more vertical vectors propagating in the opposite directions, as often encountered in simulations of the disk-stacking model (see Part I Fig. 13b). Bottom: a different *Cedrus libani* cone, uvideo-unrolled. The ontogenetic analysis reveals that it starts (Level A) from a Fibonacci (13, 21) pattern, then quickly changes to (16, 21) with three triangle transitions. Two of these transitions are canceled by pentagons aligned with them, then reappear, and are canceled again. This type of fluctuations are typical of irregular patterns getting slowly more regular, as an analysis of the disk model reveals (1, 21). Then there is a large transition zone, with three triangles and a pentagon in the opposite direction, leading to (17, 20) at Level B. This is a clear convergence toward a quasi-symmetric state. The triangle close to a pentagon in the opposite direction is typical of this process, as described in Part I. Two of the triangles are canceled by two pentagons leading back to (15, 20). Then, three pentagons yield at Level C the numbers (15, 17). Finally, as the cone reduces its size, one pentagon transition in each direction yields (16, 14) at Level D.

originate the pattern from a very strange 2×(1, 7), in other, classical words, the bijugate of a very accessory (and improbable) sequence.

In conclusion, many parastichy numbers pairs become possible if one does not tie their genesis to the zoo of the classically accepted Fibonacci-like sequences. As seen in Part I, quasi-symmetric patterns are those that systematically break the Fibonacci addition rule.

Comparison with disk accretion model

The main predictions of the disk-stacking model, namely the golden ratio scenario when the pattern is regular enough and the prevalence of quasi-symmetric patterns in presence of irregularity, are validated here, at least by a few examples. But the model is validated in more subtle ways by the observations. Indeed, when the phyllotactic

patterns are observed with precision, and in particular in the details of their irregularities, as we did above, many details appear that are perfectly coherent with the disk-stacking model.

Irregularity. The very first observation is that entirely regular patterns may not exist. Even the most regular pine cone we could find presents some irregularities, as revealed by the crystallographic and ontogenetic analysis (see Fig. 5), and so does the cabbage in Fig. 2 with its perfect increase in Fibonacci numbers, or the artichoke and its quasi-perfectly monotone decrease in Fibonacci parastichy numbers (Fig. 3). This means that the ontogeny of the plant really follows a dynamical process where the new primordia position is determined one by one by the position of the previous ones, as Hofmeister proposed [19], and that there is no general organization imposed, as a target divergence angle, even for a given parastichy number pair. The recurrence of these irregularities in plants even disqualify other dynamical systems, with very "soft" particles for instance (as were among other simulated in [21]).

Indeed large softness implies involving primordia further away than those in closest contacts in the positioning of the new ones. These models have a tendency to regularize the pattern, the softer, the quicker the regularization is. There still could be some effective softness in plants, but the persistence of irregularities, even after the pattern has converged to a rhombic tiling, shows that this is not a very large one, and that the geometry of hard disks stacking seems to be a better approximation.

Propagation of vectors. One detail in favor of the dynamical stacking of hard disks is the propagation of vectors of a given direction (up or down) along a parastichy in the opposite direction. When one front vector is very different from the other ones in the same direction, more vertical or more horizontal, it is visible as a step in the corresponding parastichies. Due to the tilling of rhombi, this step (vector) will propagate in the other direction, forming a staircase, as in Fig. 13b of Part I. Such propagation, already noted in model and specimens in [22], is visible in several of the analyses presented here. It is visible even in the most regular pine cone, shown in Fig. 5, thanks to the very precise crystallographic analysis. Such propagation around the square transition, revealed by the crystallographic analysis, is also visible in the two other pinecones (Fig. 6 and Fig. 7), even if they are much more irregular. Such staircases are also directly visible on the side view of the *Cedrus libani* male cone in Fig. 8, or on the birch catkin (Fig. 4).

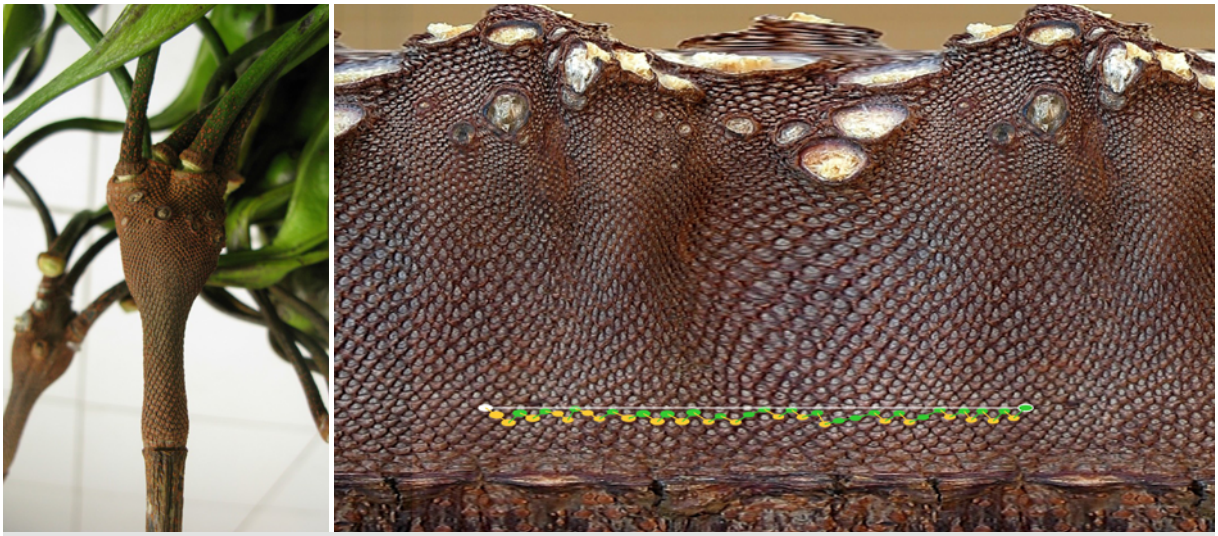

Fig. 9 Peteh (*Parkia speciosa*) inflorescence (from Bogor) Left: a side picture. One can see on top the beginning of the young pods containing the green bean favored in Indonesian cooking. Right: an unrolled stem. The flattened expanded upper part and grown pods leads to strong deformation of the pattern, both in reality and in the video projection. However, a (22, 21) pattern is clearly visible at the base. Its large irregularity is seen at the irregular alternation of up and down vectors at the front and the formation of relatively large groups of them, despite their almost equal total numbers. To better visualize the front its elements have been drawn with a large ellipse of the color of the ending vector.

Triangle–pentagon pairs. The same effect of vector propagation in the opposite direction is also visible in the ontogenetic graph, with the triangle–pentagon pairs. As said in Part I, these pairs which change the number of parastichies in one direction before changing it back to the original numbers, have for effect to regularize the pattern (through the pentagon transition) (Golé and Douady, unpublished manuscript "Convergence in a disk-stacking model on the cylinder"). When the pattern is not too disturbed, the pairs can be easily associated, and they are linked along the direction of the unchanged parastichies. This is already visible as three connected triangle–pentagon pairs in the numerical simulation of a Fibonacci transition with noise, in Fig. 1b. One observes such a localized pair in the ontogenetic analysis of the artichoke inflorescence (see the red triangle in Fig. 3, right, on top). In this case, as it is a decreasing parastichy number sequence, one observes the reverse pentagon–triangle pair.

The best example of triangle–pentagon pairs is in the analysis of the *Cedrus libani* male cone. In that example, one can observe six nicely aligned pairs. This is consistent with the fact that this pattern is more irregular, and triggers regularization mechanisms. This is also shown in the similar numerical simulation of Fig. 10. In this case, we observe many regularizing pairs, either triangle–pentagon, in the direction that is globally increasing its parastichy number while converging toward a more symmetric state, while it is reverse, pentagon–triangle, in the direction that is reducing its parastchy number. When the two elements of the pairs are separated, this creates propagating stairs discussed above, but limited between the two transition points.

Note that in the case of quickly decreasing/increasing relative primordia diameter, the pairs are not observed, as there are new transitions happening before the opposite transition can take place. This corresponds to Part I Fig. 13a, during the first part of diameter reduction. This explains also why such pairs are not observed in the quickly decreasing parastichy numbers of the pinecones.

Positions of the transitions. From a crystallographic point of view, the change in parastichy numbers is necessarily associated with the corresponding number of dislocations. The main result of Part I, in the sufficiently regular cases, is to explain why we have the right Fibonacci number of such dislocations (triangles/pentagons for rising/decreasing parastichy numbers respectively).

A further prediction of the model is that the transitions of a front become spread out to a larger area of the pattern when noise is introduced (as in Fig. 1b, bottom). This is what the ontogenetic graphs of the plant patterns shown here confirm. When the spread is small one finds the same alignments as for the pairs and square stairs

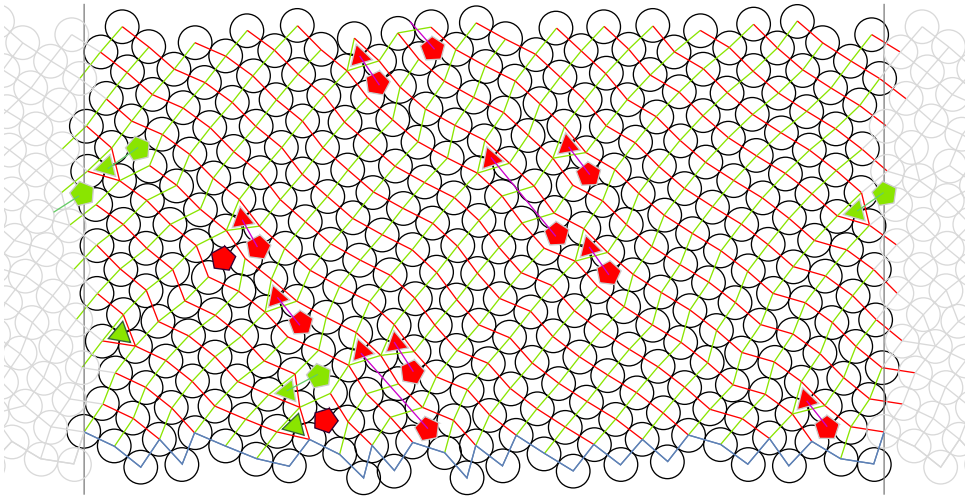

Fig. 10 Simulation showing a drift from Fibonacci to quasi-symmetric from a Fibonacci (13, 21) pattern, that quickly changes to (14, 18) with one triangle and three pentagons. After two of the first pentagons are canceled with triangles. There are also many pentagon–triangle pair in one direction, triangle–pentagon pair in the other. But one triangle and one pentagon are left alone. This, thus, lead to a globally (15, 19) pattern, with regularizing fluctuations (pairs).

along the opposite parastichy, as in the upper part of Fig. 1b. In the front of a lattice with Fibonacci parastichy numbers, there can be at most two vectors of one kind in a row. In a very regular pattern undergoing slow enough transitions, we would expect these (more horizontal) vectors in the pairs to fill in with triangles – the transitions occurring on all vectors of a type in the same front. This ideal case results in triangles either isolated or grouped by pairs, as in Fig. 1a. Seeing three triangles in a row along a parastichy is therefore a sign of a moderate spread of the transitions. When there are alignments of transitions, one also observes, between groups of transitions, parastichies making sharp turns but with no triangle, or pentagon transitions, as in the first transition (bottom) of the simulation of Fig. 1b.

Such an alignment of triangle transitions is visible in Fig. 2a (top), and for the very regular pine cone, Fig. 5, where an alignment of three triangles is observed in both case. For larger irregularities, the alignments become stronger, as they are very visible in the pentagons of the artichoke Fig. 3, where many pentagons align in groups of three.

Shift towards quasi-symmetry. The cedar male cone sample is exemplifying the model and its result. It shows that in the case of large irregularity, even when starting from Fibonacci numbers of parastichies, there is a shift toward a quasi-symmetric state. In particular, the occurrence at the same place of a triangular transition in the direction of the smaller number of parastichies, and a pentagon in the direction of the larger one, shows in a real botanical example the essential mechanism bringing the irregular states toward the quasi-symmetric one.

The peteh inflorescence stem also show that in the case of too quick decrease of the relative size of the primordia to the circumference, one directly converge toward a quasi-symmetric state. In this case, the stem presents four involucral bracts, and then very small flowers. However, the transition is not instantaneous and careful inspection (see supplementary material) shows flower bracts that are first large but reducing their size quickly.

Conclusion

In this article, we show, as in Part I [1], that the real complexity of botanical patterns can be tackled. Instead of looking at idealized systems, with observations reduced to few numbers, or to one sequence of apparently meaninglessly fluctuating numbers such as the divergence angles, one can not only describe in simple geometric terms the classical Fibonacci phenomenon when the pattern is regular enough but also observe and characterize the irregularities and their consequences. In our observations, we took care of going back, in as much as possible to the original stacking of the infant primordia, either by looking at the juvenile patterns under microscopy, or inverting the effect of the secondary growth by consistently keeping track of contacts between botanical elements.

From these contacts, one can reconstruct the ontogenetic graph, and study its transitions. The local transition tiling, with either triangles or pentagons, their positioning and especially their spreading along coherent lines in the presence of irregularity, are good evidence of an iterative accretion process of hard elements in the formation of these botanical patterns.

One can further use the full details of the contact, including the smaller ones, to extend the ontogenetic graph to the crystallographic one. Although this method is sensitive around the region of square packing of the pattern where transitions in secondary parastichies take place, which is not ontogenetically meaningful, it also reveals, as in the stacking model, the propagation of irregularities along the opposite parastichy direction, similar to the development of "stairs".

In this second part, we studied several examples of real patterns in detail, and showed how these details reveal the underlying process of their formation. In a future article, we will make more general observations on families of plants, and will have more general discussions about the conditions under which the different cases occur. This will show a broad adequacy of the disc accretion model, and in particular its

ability to distinguish between two possible broad types of patterns, the golden ratio ones and the quasi-symmetric ones, with botanical reality.

Finally, we can say that with these detailed geometric tools, and the ones developed in the first part, one can finally dive into the details of the reality of the formation of the phyllotactic patterns, and in particular their transitions. This is a big departure from so many studies where only the mathematical properties of the Fibonacci numbers, or of the Fibonacci rule, were used to fantasize about the reasons for their occurrence in plants. Here we see that the unavoidable presence of irregularities is prevalent. And within this irregular real world, it is the coherence between the local transitions that allows the particular patterns to appear.

Acknowledgments

The authors are deeply grateful to Jacques Dumais for inspiring and supporting this work, for many fruitful debates, and for providing the electron micrograph of the artichoke inflorescence.

Supplementary material

The following supplementary material for this article is available at http://pbsociety.org.pl/journals/index.php/asbp/rt/suppFiles/asbp.3534/0:

Appendix S1 Euler's polyhedral's formula and the mean number of neighbors of a cell.

Fig. S2–Fig. S4 Supplementary figures on *Cedrus*, *Parkia*, and *Pinus*.

Fig. S5–Fig. S13 Original pictures of the specimens, from both articles (Part I and Part II), before being drawn on.

References

1. Golé C, Dumais J, Douady S. Fibonacci or quasi-symmetric. Part I: why? Acta Soc Bot Pol. 2016;85(4):3533. https://doi.org/10.5586/asbp.3533
2. Hotton S, Johnson V, Wilbarger J, Zwieniecki K, Atela P, Golé C, et al. The possible and the actual in phyllotaxis: bridging the gap between empirical observations and iterative models. J Plant Growth Regul. 2006;25:313–323. https://doi.org/10.1007/s00344-006-0067-9
3. Fierz V. Phyllotactic patterns in cones of conifers. Acta Soc Bot Pol. 2015;84(2):261–265. https://doi.org/10.5586/asbp.2015.025
4. Guédon Y, Refahi Y, Besnard F, Godin C, Vernoux, T. Pattern identification and characterization reveal permutations of organs as a key genetically controlled property of post-meristematic phyllotaxis, J Theor Biol. 2013;338:94–110. https://doi.org/10.1016/j.jtbi.2013.07.026
5. Hamant, O, Heisler MG, Jönsson H, Krupinski P, Uyttewaal M, Bokov P, et al. Developmental patterning by mechanical signals in *Arabidopsis*. Science. 2008;322:1650–1655. https://doi.org/10.1126/science.1165594
6. Douady S, Couder Y. Phyllotaxis as a self organizing iterative process, Part III: the simulation of the transient regimes of ontogeny. J Theor Biol. 1996;178:295–312. https://doi.org/10.1006/jtbi.1996.0026
7. Zagórska-Marek B. Phyllotaxis triangular unit; phyllotactic transitions as the consequences of the apical wedge disclinations in a crystal-like pattern of the units. Acta Soc Bot Pol. 1987;56:229–255. https://doi.org/10.5586/asbp.1987.024
8. Atela P, Golé C. Rhombic tilings and primordia fronts of phyllotaxis [Preprint]. 2007 [cited 2016 Dec 30]. Available from: http://arxiv.org/abs/1701.01361
9. Plantefol L. La théorie des hélices foliaires multiples. Paris: Masson; 1948.
10. Meicenheimer RD. Role of parenchyma in *Linum usitatissimum* leaf trace patterns. Am J Bot. 1986;73(12):1649–1664. https://doi.org/10.2307/2444231
11. Zagórska-Marek B. Phyllotaxic diversity of *Magnolia* flowers. Acta Soc Bot Pol. 1994;62(2):117–137. https://doi.org/10.5586/asbp.1994.017

12. Sadoc JF, Rivier N, Charvolin J. Phyllotaxis: a non conventional crystalline solution to packing efficiency in situations with radial symmetry [Preprint]. 2012 [cited 2016 Dec 30]. Available from: https://arxiv.org/abs/1201.1432
13. Rivier N, Sadoc JF, Charvolin J. Phyllotaxis: a framework for foam topological evolution The European Physical Journal E. 2016;39:7. https://doi.org/10.1140/epje/i2016-16007-8
14. van Iterson G. Mathematische und mikroskopisch-anatomische Studien über Blattstellungen nebst Betrachtungen über den Schalenbau der Miliolinen. Jena: Gustav Fischer Verlag; 1907. https://doi.org/10.5962/bhl.title.8287
15. Adler I. A model of contact pressure in phyllotaxis. J Theor Biol. 1974;45:1–79. https://doi.org/10.1016/0022-5193(74)90043-5
16. Douady S. The selection of phyllotactic patterns. In: Jean RV, Barabé D, editors. Symmetry in plants. Singapore: World Scientific; 1998. p. 335–358. (Series in Mathematical Biology and Medicine; vol 4). https://doi.org/10.1142/9789814261074_0014
17. Atela P, Golé C, Hotton S. A dynamical system for plant pattern formation: a rigorous analysis. Journal of Nonlinear Science. 2002;12:641–676. https://doi.org/10.1007/s00332-002-0513-1
18. Lagesse C, Bordin P, Douady S. A spatial multi-scale object to analyze road networks. Netw Sci (Camb Univ Press). 2015;3(1):156–181. https://doi.org/10.1017/nws.2015.4
19. Hofmeister W. Allgemeine Morphologie der Gewächse. In: du Bary A, Irmisch TH, Sachs J, editors. Handbuch der Physiologischen Botanik. Leipzig: Engelman; 1868. p. 405–664.
20. Couder Y. Initial transitions, order and disorder in phyllotactic patterns: the ontogeny of *Helianthus annuus*: a case study. Acta Soc Bot Pol. 1998;67(2):129–150. https://doi.org/10.5586/asbp.1998.016
21. Douady S, Couder Y. Phyllotaxis as a self organizing iterative process, Part II: the spontaneous formation of a periodicity and the coexistence of spiral and whorled patterns J Theor Biol. 1996;178:275–294. https://doi.org/10.1006/jtbi.1996.0025
22. Zagórska-Marek B, Szpak M. Virtual phyllotaxis and real plant model cases. Funct Plant Biol. 2008;35:1025–1033. https://doi.org/10.1071/FP08076